

## Features of using a railgun in problems of high-speed interaction of bodies with obstacles

© M.A. Yadrenkin, V.P. Fomichev, A.A. Golyshev

Khristianovich Institute of Theoretical and Applied Mechanics, Siberian Branch, Russian Academy of Sciences, 630090 Novosibirsk, Russia  
e-mail: yadrenkin@itam.nsc.ru

Received October 25, 2023

Revised December 12, 2023

Accepted December 21, 2023

Examples of the use of a rail mass accelerator (railgun) as part of a multifunctional ballistic complex designed to solve problems of high-speed interaction of bodies with obstacles are shown. A description is given of methods for accelerating micro- and macro-scale bodies inside a dielectric container driving through a channel by plasma piston. The results of tests of metal-ceramic coatings formed by laser cladding are presented. It was shown that gas-dynamic effects have a significant influence on the nature of the acceleration of the powder mixture of microparticles. The possibility of using a vacuum chamber to conduct experimental studies of the impact interaction of microparticles with obstacles at low ambient gas pressure has been demonstrated.

**Keywords:** rail mass driver, plasma piston, microparticles, vacuum chamber, ballistic track.

DOI: 10.21883/0000000000

### Introduction

Modern scientific and technological problems associated with the processes of high-speed impact interaction of solid deformable bodies require the development of experimental and numerical methods for studying the behavior of materials under high-energy pulse loading conditions. The relevance of such research is beyond doubt. These tasks include research into the mechanical characteristics of new materials and coatings to protect various objects from mechanical impact. For example, protection of spacecraft elements from space enterings or dust [1,2], impact interaction of cosmic bodies [3] and many others [4–7]. It is worth noting that in practice, the process of impact interaction between a body and an obstacle manifests itself in a complex of various physical phenomena: significant deformations and destruction, thermophysical transformations, changes in the structural and phase composition of the substance, and accompanying gas and hydrodynamic effects. This is determined by the clear priority of experimental data in the applied aspect of their use.

In this work, methodologies for accelerating micro- and macro-sized bodies in the channel of a rail electrodynamic mass accelerator are considered to implement experimental studies of high-speed interaction of solid deformable bodies of various sizes under various environmental parameters.

### 1. Ballistic bench for studying high-speed interaction of bodies based on a rail mass accelerator

It is obvious that the experimental study of processes of high-speed interaction of bodies requires the creation

of special installations and corresponding methodologies for accelerating bodies, as well as the development of modern methods for studying fast high-energy processes under given interaction parameters. To achieve high speeds of collision of bodies with obstacles (more than 1000 m/s), various ballistic installations can be used in the experiment, i.e. devices for accelerating objects in order to study their movement along a ballistic trajectory under conditions of interaction with substances of various physical nature [8–10]. Electrodynamic accelerators of objects, the operation of which is based on the conversion of electrical energy into the kinetic energy of a projectile, make it possible to overcome the main limitation of the maximum achievable speed of body movement associated with the sound speed of the gas in the channel. Among the electrodynamic accelerators of bodies, can be distinguished i.e. railguns. This class of installations allows the acceleration of bodies of various masses ( $10^{-4}$ – $10^{-2}$  kg) to speeds over 5000 m/s [11–15]. According to the authors of this work, the use of railguns is a promising way to implement the conditions for high-speed collisions of bodies when solving applied and fundamental problems such as the impact interaction of bodies with obstacles, the penetration of micro-impactors into metals, the creation and destruction of coatings of various physical natures (including heterogeneous ones), phase transformations of substances during impact interaction and others.

The installation based on a railgun consists of the rail accelerator itself, a power source and a ballistic track. As a rule, the railgun channel is formed by two dielectric surfaces and a pair of conductive ones the rails. The principle of operation of a rail mass accelerator is to convert electrical energy into the kinetic energy of an accelerated object with electrically conductive properties under the

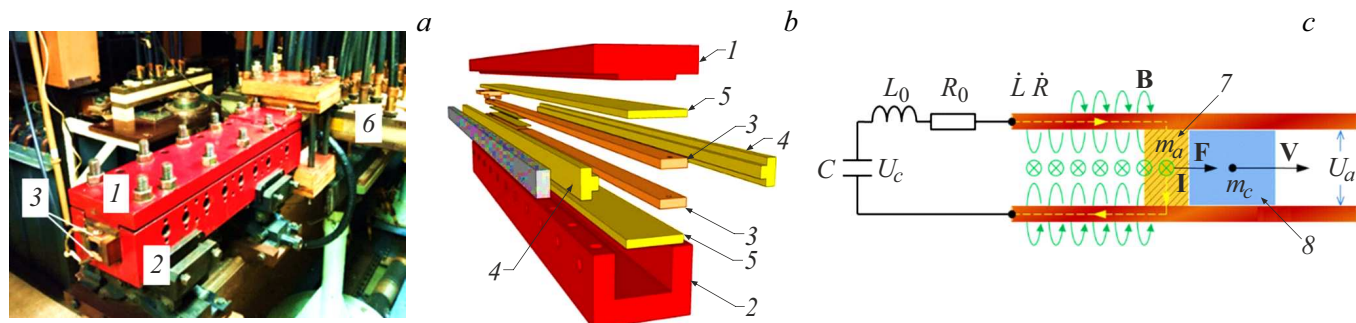


**Figure 1.** General view of the railgun (a), assembly of channel parts (b) and diagram of the railgun with a plasma piston (c). 1 — cover, 2 — casing, 3 — electrodes, 4, 5 — isolators, 6 — current collector, 7 — plasma piston, 8 — accelerated body.

influence of electromagnetic force that occurs when a strong electric current passes through the operating circuit, obtained using high-capacity capacitor batteries, or using magnetic explosion generators [16]. During the acceleration process in the railgun channel under the influence of the Ampere force, the accelerated body encounters substantial resistance to movement due to various factors. These include the gas-dynamic grad caused by the gas expelled from the channel, the friction resistance between the body and the channels walls, and the kinematical resistance resulting from the increased mass of the plasma piston and the overall mass due to continuous thermal ablation of the electrode surface [17,18]. Despite the low efficiency (usually about 10%), this method makes it possible to accelerate bodies of various geometries up to speeds of several kilometers per second in a relatively short channel (of the order of 1 m), which is a significant advantage compared to other types of accelerators, for example, light-gas guns [8]. Among the obvious disadvantages of the electrodynamic method of accelerating bodies, the following can be identified: mechanical wear of the channel, as well as the presence of combustion and melting products of the channel walls, the movement of which after the accelerated object can negatively affect both the result of the experiment and the diagnosis of the observed phenomena. However, the absolute characteristics of this class of installations in some cases determine this method of accelerating bodies as the only one possible for realizing unique experimental conditions.

The railgun, developed and created at the ITAM SB RAS, made according to the scheme of a V with rail accelerator plasma piston, is presented in Fig. 1. The two opposite walls of the rectangular channel are formed by massive copper electrodes, and the other two walls are made of fiberglass are formed by durable dielectric composite material with good wear resistance. After assembly, the channel is calibrated using a special tool, and at the blind end there is a strip of copper foil touching the rails. When a powerful electrical pulse is applied to the electrodes, an electric explosion of

the foil occurs, resulting in the formation of a plasma piston. So that in this case, to withstand a pressure surge up to values of the order of 10 MPa [19], the railgun channel is enclosed in a steel casing. Depending on the chosen acceleration method and the required experimental parameters, the length of the channel can vary from 0.5 to 1 m, and its cross-section — from  $10 \times 10$  to  $18 \times 18$  mm.

The power supply system of the rail accelerator consists of 5 series-connected sections of high-voltage capacitors with a total capacity of 0.04 F. At a maximum voltage of 5 kV, the current flowing through the plasma piston can reach 550 kA, and the maximum stored energy in the battery is about 0.5 MJ. If it is necessary to generate a current pulse of a certain profile and duration, the capacitor banks can be switched on not simultaneously, but alternately with a specified time interval. This available power of ballistic installation based on a railgun makes it possible to accelerate bodies of various masses in a wide range of supersonic speeds (Fig. 2).

## 2. Methodologies for accelerating bodies in a railgun channel

Various methodologies for accelerating bodies in the railgun channel and ensuring their movement along the entire length of the ballistic track are intended to ensure the necessary conditions for conducting the experiment. As a rule, in works devoted to experimental studies of high-speed interaction of bodies, more attention is paid to the description of the physical processes of impact interaction and, to a lesser extent, to the features of methods for achieving research results. In connection with this, difficulties may arise when attempting to repeat or confirm the result by independent teams of authors. There is no doubt that both the result itself and the correctness of the interpretation of the observed phenomena depend on the methodology of the experiment.

When accelerating bodies in a railgun, various patterns of electric current flow through the accelerated object are

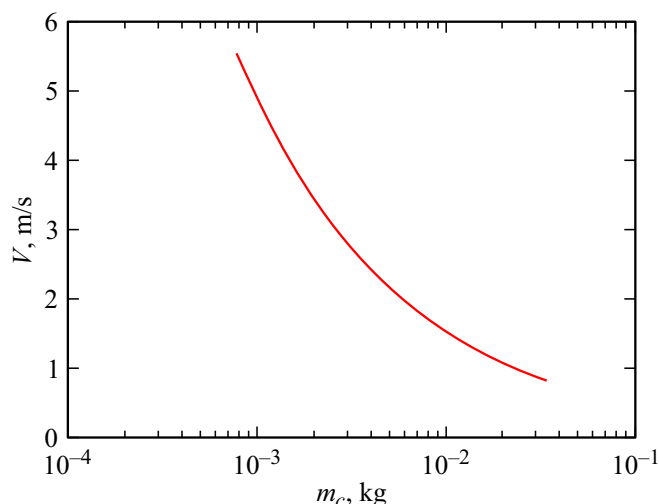


**Figure 2.** Achievable speed of subjects of various masses in the railgun of the ITAM SB RAN.

possible. In case, if the accelerated body is electrically conductive, then its acceleration occurs when an internal electromagnetic force occurs, formed when current flows directly through the body when it is in close contact with the rails. The accelerated body can be made of a dielectric material, while the flow of current must be realized through a plasma piston, which, accelerated by electromagnetic force, creates pressure on the body, causing it to move. The first method is applicable in those experiments where the preservation of the shape and properties of the accelerated object is not so important, and a small loss of mass due to melting of the metal in the contact area does not introduce a significant error in the research results, or the accelerated body is a load-bearing metal container with an object enclosed in it target of research. The disadvantage of this method is also that the accelerated object must be made exactly according to the cross-sectional shape of the channel, which leads to difficulties in manufacturing either the body in the case of using a rectangular channel, or the channel itself when an object of cylindrical shape is accelerated.

The use of a plasma piston makes it possible to accelerate free form bodies by placing them in a dielectric container. The formation of a plasma piston occurs during the electric explosion of a thin metal conductor, for example, a strip of copper foil, at the moment of passage of a strong electric current through it with the release of Joule heat at the beginning of the electrical discharge [20,21]. The plasma piston exerts significant pressure on the accelerated object both due to the thermal expansion of metal vapor and as a result of the occurrence of electromagnetic force in the conductive circuit. Any dielectric capable of withstanding the loads encountered during acceleration can be used as the material of the accelerated body (container). The main advantage of this technique is the absence of electrical contact of the accelerated body with the walls of the channel, as well as the absence of significant heating of the

body and its thermal deformations at the time moment of acceleration. In this way, it is possible to accelerate both a single target and a group of targets, which is necessary when studying their joint high-speed influence on the deformation of an obstacle.

When studying the process of collision of a body with an obstacle, it is necessary to ensure their interaction in a given speed range, preserving the integrity of the accelerated object up to the moment of contact. These conditions can be achieved by accelerating a test sample in a dielectric container by using a plasma piston. However, despite the fact that the density of the container may be several times less than the density of the striker element, and its mass, as a rule, exceeds the mass of the body, and the container hitting the obstacle leads to significant deformations of the target. To eliminate the influence of the container on the interaction process, methodics were implemented to accelerate bodies with separation of the container either aerodynamically or mechanically. A schematic representation of the main stages for the movement of bodies along a ballistic path is presented in Fig. 3.

This work presents examples of the use of techniques for accelerating micro- and macro-striker elements at different ambient air pressures, implemented at the experimental stand of the ITAM SB RAS.

## 2.1. Throwing bodies in a split container

Acceleration of macro striker elements with a diameter of up to 5 mm was carried out in a split container according to the diagram in Fig. 3, *a*. The container design consisted of two identical halves, which have an aerodynamic shape that, after the container leaves the channel, leads to its opening under the influence of forces and moments created by the pressure of the oncoming air flow (Fig. 4).

The stages of acceleration and passage of the accelerated body on the ballistic path are presented in Fig. 3, *a*, where I — the initial position of the body in the container, II — the acceleration of the container with the body in the channel at a pressure of the plasma piston, III — the phase of separation of the container under the action of aerodynamic forces and the formation of a shock wave structure, IV — the moment of stopping the halves of the container using a cutting device, V — the interaction of the body with the obstacle.

The container must be made of a material with sufficient impact strength to withstand both the pressure of the plasma piston and the pressure of the accelerated body on its bottom. For the material of an accelerated object, there are also certain strength limitations caused by the deformation of the body by the acceleration force, the magnitude of which can reach the order of  $10^5$  G.

Measuring the speed of the striker element can be realized in various ways: by flying a container through a target frame (a system of thin metal grids threads closed to a measuring circuit), or using high-speed video filming of the process of a body flying in close proximity to an

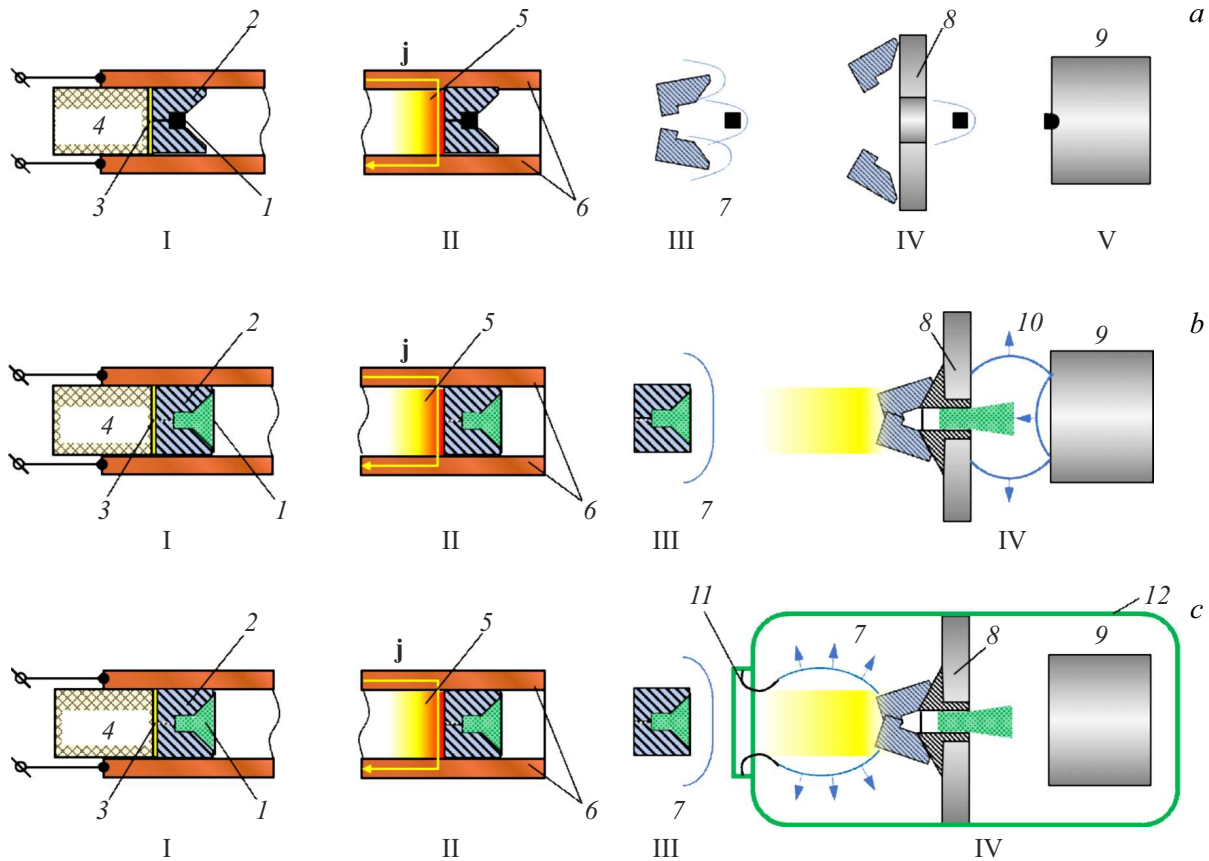


**Figure 3.** Acceleration stages of macro-striker elements in a separating container (a) [22] and microparticles in a solid container in the atmosphere (b) [23] with a vacuum chamber (c). 1 — accelerated body, 2 — container, 3 — copper foil, 4 — shutter, 5 — plasma piston, 6 — rails, 7 — diagram of the SWS flow near the container, 8 — cutting device, 9 — target, 10 — diagram of the SWS flow in the interaction region, 11 — membrane, 12 — vacuum chamber.

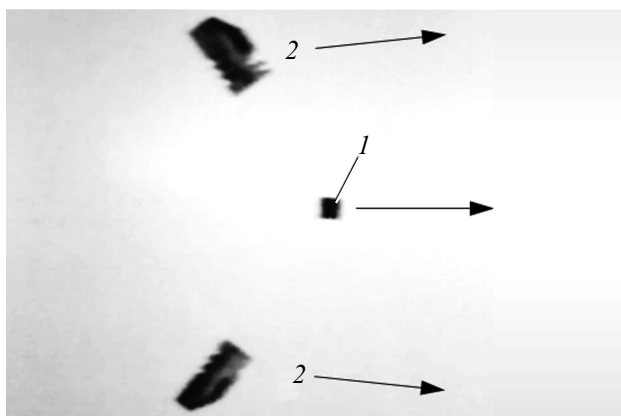


**Figure 4.** Disclosure of the container and the direction of flight of the accelerated parts of the projectile. 1 — cylindrical striker element, 2 — container parts.

obstacle while fixing the position of the accelerated object relative to a scale bar. Knowing the frequency of shooting, the exposure time of the frame and the distance traveled by the body, it is possible to determine the speed of the striker

with an accuracy of 5%, depending on the experimental conditions.

The works [22,24,25] present the results of a wide range of experimental studies of the high-speed impact resistance of various coatings created by laser additive printing methods. Tests were carried out for both metallic and metal-ceramic coatings. In addition, the question of the influence of the type of reinforcement (particles or discrete fibers) of the coating on the nature of destruction during interaction with an accelerated body was considered.

In the works presented above, a ball with a diameter of 4.8 mm and a weight of 0.5 g, made of hard steel ShKh15, was used as an accelerated body. The velocity of the striker-element was determined using a Photron Fastcam SA-Z high-speed video camera. Fig. 5 shows video footage of the interaction of a spherical striker element made of ShKh17 hard steel with a Ti64-SiC metal-ceramic coating at a speed of 1165 m/s. The figure shows that after the collision, the coating material in the impact area is destroyed and fragments scatter.

Figure 6 shows photographs of the coating before and after high-speed impact testing of metal-ceramic coatings based on titanium: a, d — pure titanium Ti64; b, e — Ti64

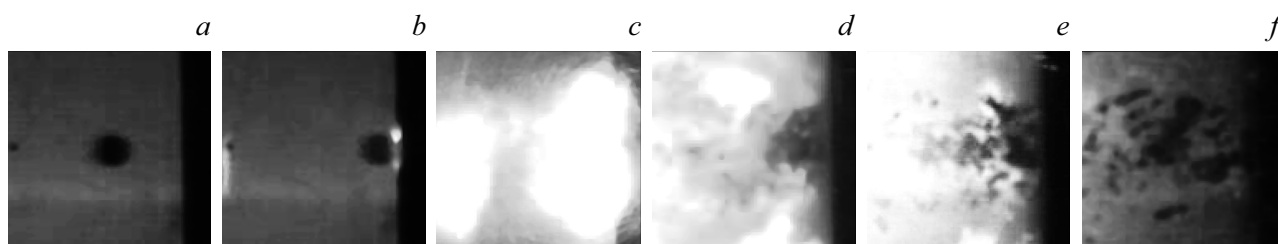


**Figure 5.** Collision of the striker element with a metal-ceramic coating at initial speed of 1165 m/s after 3 (c), 60 (d), 97 (e) and 263  $\mu$ s (f) after the start of interaction (b).

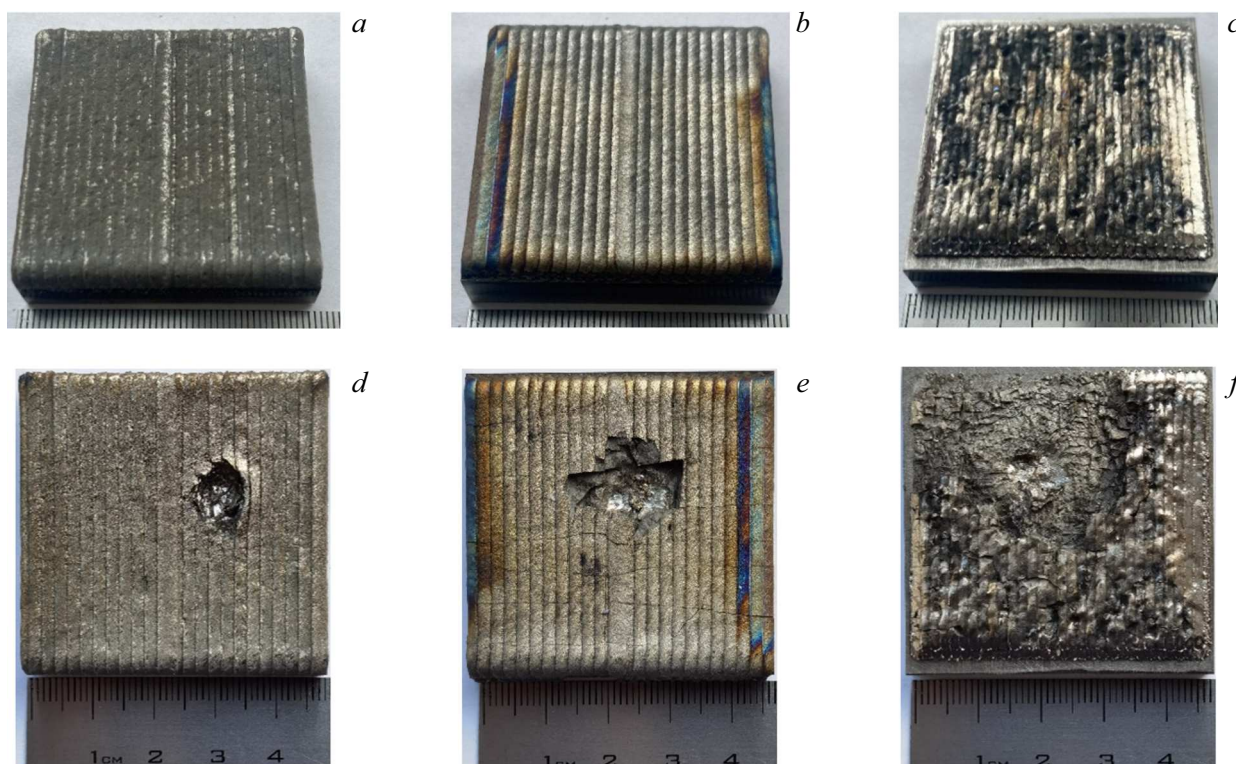


**Figure 6.** Photos of the coating before (a, b, c) and after (d, e, f) [24,25] high speed impact test.

with SiC powder in a ratio of 9:1 mass.%; c, f—Ti64 and crushed SiC fiber in a ratio of 1:1 vol.%. It can be seen that as a result of the interaction of the striker element with the coating, a crater with different types of destruction is formed.

It was found that the ceramic-free coating after testing has a cylindrical crater with smooth edges (Fig. 6, d), and with the high-speed interaction of the impactor with the metal-ceramic coating, the deposited layer along the perimeter of the crater is destroyed. Moreover, for a coating with ceramic particles, destruction occurs in the form of a hole with crumbling (Fig. 6, e), and for a coating with ceramic fiber, destruction occurs in the form of disk formation (Fig. 6, f).

When determining the crater depth, it was found that for sample Ti64-SiC powder, the crater depth is 1437  $\mu$ m. In the case of using discrete ceramic fibers, the depth of the crater in the coating decreased by 22% and amounts to

1137  $\mu$ m. The results obtained allow us to conclude that the coating with fibers provides more efficient dissipation of the kinetic energy of the striker element throughout the entire volume of the sample, and not just near the control point of the striker element.

## 2.2. Throwing of microparticles placed in container

Using a container to disperse bodies allows you to place both single objects and a group of objects into it. A special case is the problem of interaction of a powder mixture of particles with a diameter of several micrometers with a solid barrier. The complexity of organizing such an experiment lies in the separation of the stage of particle acceleration in the container and the stage of their free flight along the ballistic path before interacting with the obstacle. The use of the methodology for accelerating bodies with

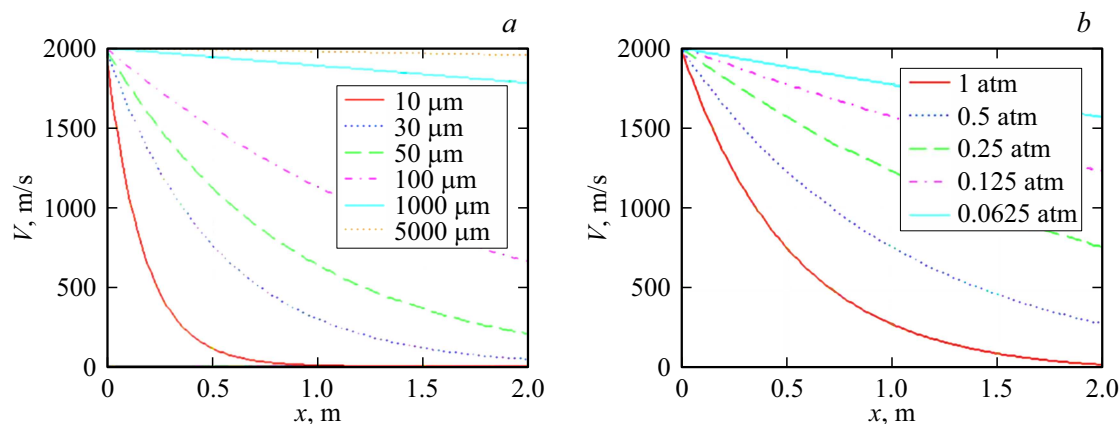


**Figure 7.** Change in the speed of a microparticle depending on its size and environmental pressure.

a separating container is not applicable at atmospheric pressure of the surrounding air, since the aerodynamic drag acting on light microparticles begins to play a critical role. When the particle diameter is less than 100  $\mu\text{m}$ , there is a significant drop in their speed with each centimeter of distance traveled. For example, at an initial speed of 2000 m/s, particles with a diameter 100  $\mu\text{m}$  will lose their speed by half after 1.2 m free flight, and particles with a diameter 10  $\mu\text{m}$  will lose it after 0.12 m. Fig. 7 shows the dependence of the speed of spherical particles of different diameters moving in atmospheric air pressure (Fig. 7, *a*) and for a particle with a diameter 30  $\mu\text{m}$  at different ambient air pressure (Fig. 7, *b*). Estimates were carried out for the case of flow around an individual particle. The graph shows that in order to ensure a given speed of particles with a diameter less than 100  $\mu\text{m}$ , it is necessary to ensure either a short distance of movement of microparticles after their departure from the container volume, or to reduce the air pressure to values of the order of 1000 Pa and below. It is worth noting that during the group movement of microparticles, the resulting two-phase flow will probably experience less gas-dynamic resistance. However, with the observed expansion of a supersonic two-phase jet consisting of gas and microparticles, the hydrodynamic resistance of individual microparticles will have more and more weight. Therefore, the decrease in particle velocity will still be significant, and the presented estimates allow us to consider the influence of particle sizes and environmental pressure on the dynamics of their propagation.

A short microparticles transit distance can be achieved by using a non-separable container, stopped using a cutting device immediately before interaction with the obstacle. The container may have the shape of a prism with a deepening, and the cutting device may have the shape of a truncated cone with a through hole along the axis of symmetry. The cutting device is fixed in the wall of a massive structure installed on the flight path of the container. Since the opening of the cutting device has a diameter smaller than the dimensions of the container, but larger than the diameter of the accelerated object, the contents

of the container unhindered continue their movement in the direction of the target, while the container itself is destroyed upon impact with the cutting device. In this case, the container significantly consumes its kinetic energy, and those fragments of the container that reached the surface of the target do not lead to any significant damage to its surface. The stages of acceleration and transit of accelerated microparticles on the ballistic track are presented in Fig. 3, *b* (where I is the initial position of the particles in the container, II is the acceleration of the container with particles in the channel at a pressure on it of the plasma piston, III is the phase of the container flying along the ballistic path with the formation of a shock-wave structure, IV is the destruction of the container upon its collision with the cutting device and the transit of microparticles along the cutting device channel with subsequent interaction wave with the reflected shock wave and the target surface).

To avoid a significant loss of speed of microparticles after their transit from the cutting device, it is necessary to place the target at a distance of several centimeters [23]. Thus, it is possible to study the high-speed interaction of many microparticles with an obstacle, providing a given impact speed. However, this methodology has a number of features that can negatively affect the quality of the experiment. First of all, these include gas-dynamic shock-wave effects that arise near the target surface [26]. Before the container collides with the cutting device, a front shock wave is formed in front of it, caused by gas compression when the container moves at supersonic speed. Air compression occurs when a dense stream of microparticles passes through the cutting device. As the stream exists the channel, it creates a complex shock wave structure (SWS) within the flow. This SWS is formed as the shock wave travels towards the obstacle and subsequently reflects off it. Passing through the boundary of the reflected shock wave, the leading front of the flow of microparticles experiences increased resistance from the denser environment. In addition, particles that did not move perpendicular to the shock wave front deviate from their trajectory and either do not reach the surface or interact with it not normally

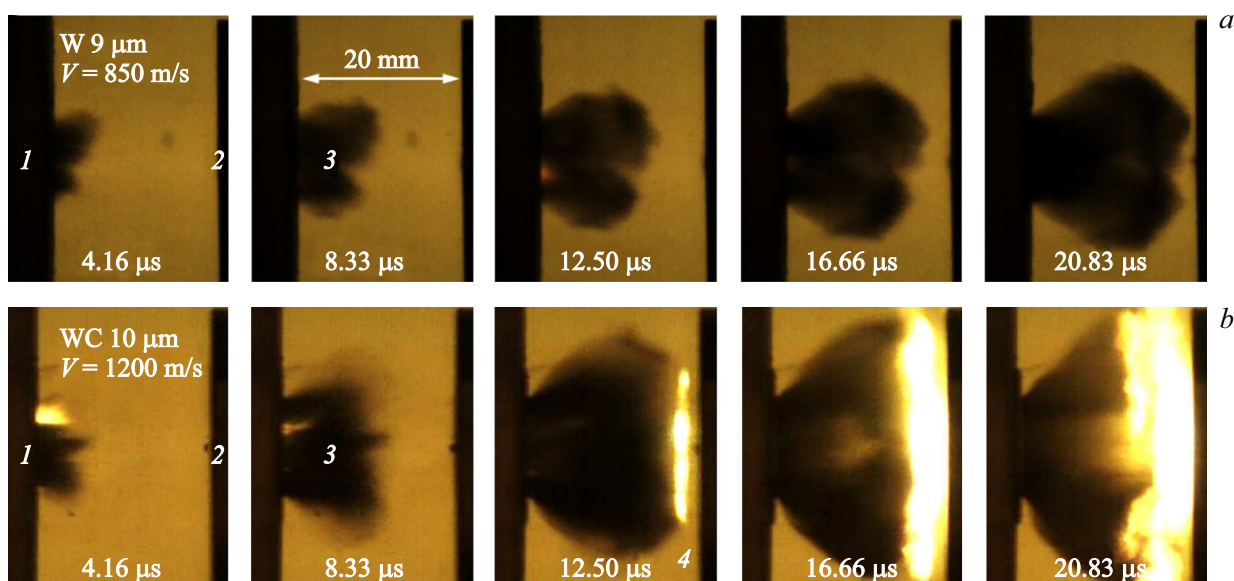


**Figure 8.** Emission of microparticles from the cutting device channel [26]: *a* — tungsten particles with a diameter of about  $9\mu\text{m}$  and an initial speed of about  $850\text{ m/s}$ ; *b* — tungsten carbide particles with a diameter of about  $10\mu\text{m}$  and an initial speed of about  $1200\text{ m/s}$ ; 1 — cutting device, 2 — target, 3 — flow of microparticles, 4 — gas glow in the region of interaction with microparticles.

and, therefore, not effectively. Fig. 8 shows frames of high-speed video recording ( $240\text{ kHz}$ ) of the emission of tungsten microparticles 3 with a diameter of about  $9\mu\text{m}$  from the cutting device channel 1 in the direction of the target surface 2 with an initial speed of  $850\text{ m/s}$  (Fig. 8, *a*) and microparticles of tungsten carbide with a diameter of about  $10\mu\text{m}$  with an initial speed of  $1200\text{ m/s}$  (Fig. 8, *b*).

The rapid movement of particles at supersonic speeds leads to the generation of shock wave as they exit the cutting device channel. This shock wave then needs to be reflected from the target surface and intersect with the flow of microparticles. At particle speeds above  $1000\text{ m/s}$ , the experiments observed a bright glow of the region 4 located at some distance from the target. To determine the possible causes of this phenomenon, assessments were made of the ongoing gas-dynamic processes and the dynamics of particle heating in a one-dimensional approximation. It has been established that the microparticles used in the work will not have time to warm up to the radiation temperature during the transit time. However, at particle speeds of  $1000\text{ m/s}$  and higher, the gas stagnation temperature on the surface of particles (determined by the transition of the kinetic energy of the flow into potential energy) moving in the gas region behind the reflected shock wave will be at least  $2000\text{ K}$ , which corresponds to the onset temperature of nitrogen molecular dissociation. Therefore, the observed glow is caused by heating of the air during the collision of a dense two-phase flow with microparticles and compressed gas behind the front of the reflected shock wave.

Thus, when particles are thrown in air at atmospheric pressure, gas-dynamic processes play a significant role, which have a significant effect on the optical diagnostics of the impact interaction of particles with an obstacle.

### 3. Acceleration of microparticles at reduced ambient air pressure

Obviously, the possibility of increasing the free flight distance of microparticles and minimizing gas-dynamic losses requires evacuation of the experimental volume, which is a technically challenging problem. It can be solved either by placing the experimental installation in a vacuum chamber, or by creating a vacuum ballistic track, to the body of which the railgun channel will be hermetically connected. The implementation of such methods requires complex and expensive technical solutions. In order to reduce the cost of the experiment, a method was developed to accelerate a container with powder as it flies through a small vacuum chamber in which a target is installed. General view of the ballistic installation with a vacuum chamber is shown in Fig. 9. The experiment setup is shown in Figure 3, *c*.

The vacuum chamber is a cylindrical container with an airlock located at the end, flying through which microparticles pass from the atmospheric environment to a zone with reduced pressure. The airlock is equipped with a thin and lightweight polymer diaphragm at its entrance. This diaphragm is designed to withstand external atmospheric pressure while air is being pumped from the working chamber. It also facilitates the smooth passage of the container without significant speed losses during the diaphragm's destruction process. Behind the diaphragm in the airlock tank the cutting device is, similar in design to that shown in the previous interaction scheme. When colliding with the cutting device, the kinetic energy of the container with powder is converted into the energy of deformation and destruction. At the same time, the

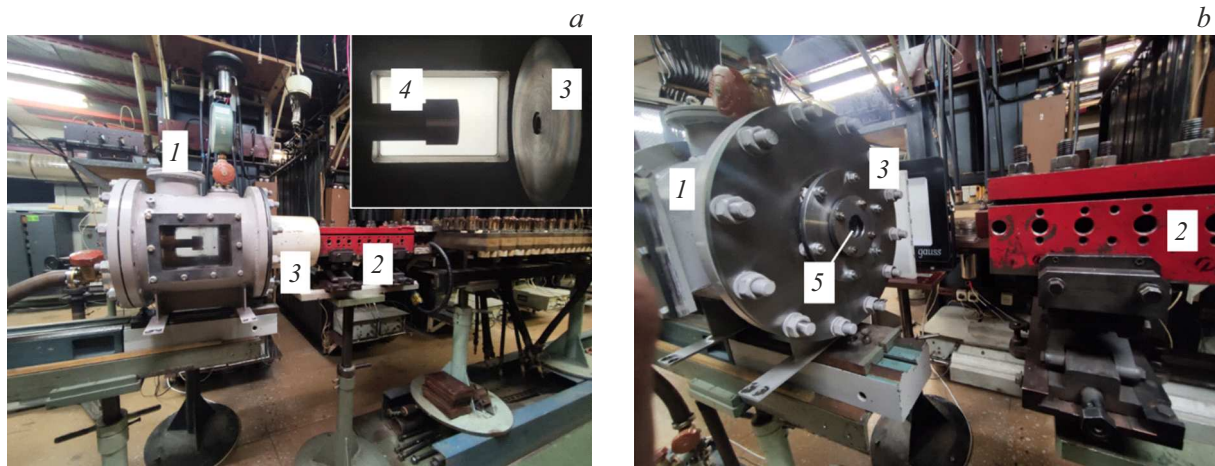


**Figure 9.** Vacuum ballistic installation based on a railgun. 1 — vacuum chamber, 2 — railgun, 3 — airlock with cutting device, 4 — target, 5 — membrane.

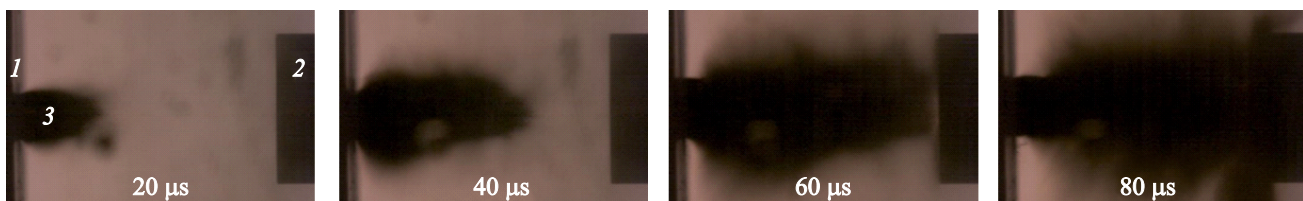


**Figure 10.** Transit of microparticles from the cutting device channel towards the target at an air pressure of 0.001 atm. 1 — cutting device, 2 — target, 3 — flow of microparticles.

microparticles continue their movement in the direction of the target. It is worth noting that, according to estimates, at a pressure drop at the entrance to the vacuum chamber of 1:1000, the speed of propagation of atmospheric air inside the chamber after the diaphragm ruptures will be about 800 m/s. Consequently, when the container moves at a higher speed, an increase in pressure near the target should be expected later than the moment the high-speed impact interaction begins. Fig. 10 shows frames of high-speed video recording (100 kHz) of the process of propagation of tungsten carbide microparticles with a diameter of about  $30\mu\text{ m}$  in the direction of the target at a pressure of about 0.001 atm. The target is made of high carbon steel. The speed of microparticles was about 1200 m/s. It has been established that the shape of the flow of microparticles differs significantly from the case of microparticles propagating in a dense air environment. The influence of external gas-dynamic processes on the dynamics of microparticle propagation is also not observed. The weak glow in the area of interaction of microparticles with the target can be explained by the conversion of the kinetic energy of particles into thermal energy with significant deformations of the particles and the target surface as a result of impact interaction.

The implemented interaction method can be used to simulate the processes of interaction of flows of microparticles with materials and coatings of various physical natures.

In practical applications, this technology can be used for experimental modeling of the process of interaction of cosmic dust with structural elements of devices in an airless environment.

## Conclusion

In this work examples of the use of a rail electrodynamic mass accelerator for solving various interdisciplinary problems are given. A vacuum ballistic installation created on the basis of a railgun makes it possible to conduct experimental studies of the stages of damage (crater formation) and the transition to target destruction during a high-speed impact.

The methodologies presented enable the acceleration of individual objects, ranging in size from tens of micrometers to several millimeters, within containers. These methodologies have been designed to work effectively across various ambient pressures. In this case, the initial properties of objects remain unchanged during acceleration until the moment of their interaction with the target.

During the testing of metal-ceramic coatings produced through laser additive printing methods, it was observed that the nature of crater formation varies based on the type of material reinforcement. This phenomenon is likely attributed to the non-isotropic dissipation of impact energy. It has been shown that coatings containing ceramic fibers

provide more efficient dissipation of the kinetic energy of the striker-element in the sample volume than coatings with particles.

During experimental studies on the high-speed interaction between a powder mixture of microparticles and obstacle, it was observed that shock-wave processes have a significant impact on the structure of the resulting two-phase flow. This influence is evident in the glowing gas behind the reflected shock wave, occurring prior to the direct interaction of the particles with the particles with the target surface.

The creation of a vacuum chamber with an inlet airlock made it possible to realize high-speed distribution of a powder mixture of microparticles in an airless environment and eliminate the influence of gas-dynamic processes on the process of their interaction with the target surface. The developed technology can be used for experimental modeling of the process of interaction of cosmic dust with structural elements of devices in an airless environment.

### Funding

This research was funded by Russian Scientific Foundation, grant number No 21-79-10213 „(<https://rscf.ru/project/21-79-10213/>). Development of scientific foundations for the creation of metal-ceramic composites by selective laser melting using ceramic fibers“.

### Conflict of interest

The authors declare that they have no conflict of interest.

### References

- [1] V.A. Kuz'min, S.I. Gerasimov, A.V. Zubankov, A.G. Sirotkina, E.P. Akasheva, R.V. Gerasimova. *Tech. Phys.*, **64** (8), 1145 (2019). DOI: 10.1134/S1063784219080103
- [2] S. Heimbs, D. Schueler, T. Bergmann, N. Toso-Pentecote. *Composite Structures*, **111** (1), 158 (2014). DOI: 10.1016/j.compstruct.2013.12.0312014
- [3] N.D. Semkin, A.V. Piyakov, A.P. Pogodin. *Prikladnaya fizika*, **4**, 153 (2018) (in Russian).
- [4] S.A. Atroshenko, A.Y. Grigor'ev, G.G. Savenkov. *Phys. Solid State*, **61** (10), 1690 (2019). DOI: 10.1134/S106378341910007X
- [5] V.G. Reyes, W.J. Cantwell. *Compos. Sci. Technol.*, **64** (1), 35 (2004).
- [6] E.I. Kraus, V.M. Fomin, I.I. Shabalin. *J. Appl. Mech. Tech. Phys.*, **61** (5), 855 (2020).
- [7] V.M. Fomin, A.I. Gulidov, G.A. Sapozhnikov, etc. *High-speed interaction of bodies* (Publishing House SB RAS, Novosibirsk, 1999) (in Russian).
- [8] N.A. Zlatin, A.P. Krasilshchikov, G.I. Mishin, N.N. Popov. *Ballisticheskiye ustanovki i ikh primeneniye v eksperimental'nykh issledovaniyakh* (Nauka, M., 1974), (in Russian). 344 p
- [9] N.D. Syomkin, K.I. Sukhachev, A.S. Dorofeev. *Elektronika, izmeritel'naya tekhnika, radiotekhnika i svyaz'*, **14** (4), 171 (2015) (in Russian).
- [10] K.I. Sukhachev, N.D. Syomkin, A.V. Piyakov. *Fizika volnovykh protsessov i radiotekhnicheskiye sistemy*, **17** (2), 49 (2014) (in Russian).
- [11] M.P. Galanin, A.D. Lebedev, A.P. Lototskiy, K.K. Milyayev. *Teplovyeye i elektromagnitnyye protsessy na kontaktakh elektrodinamicheskogo uskoritelya* (in Russian) (Preprint of the of Keldysh Applied Mathematics Institute of RAS, 2000), № 42, p. 32.
- [12] V.B. Zheleznyy, A.D. Lebedev, A.V. Plekhanov. *Vozdeystviye na dinamiku uskoreniya yakorya v REU* (in Russian). *II All-Union Seminar on the dynamics of high-current arc discharge in a magnetic field* (4–6 December, Novosibirsk, 1991), p. 16–32.
- [13] W. Witt, M. Loffler. *Military Technol.*, **5**, 80 (1998).
- [14] S.A. Ponyaev, B.I. Reznikov, R.O. Kurakin, P.A. Popov, B.G. Zhukov. *Tech. Phys. Lett.*, **45** (2), 8 (2019). DOI: 10.1134/S1063785019010322
- [15] V.E. Fortov, E.F. Lebedev, S.N. Luzganov, A.V. Kozlov, S.A. Medin, A.N. Parshikov, V.P. Polistchook, A.V. Shurupov. *Intern. J. Impact Eng.*, **33**, 254 (2008). DOI: 10.1016/J.IJIMPENG.2006.09.008
- [16] E.F. Lebedev, V.E. Ostashev, V.E. Fortov. *Megagauss Magnetic Field Generation, its Application to Science and Ultra-High Pulsed-Power Technology. EXPLOSIVE MHD GENERATORS* (2004). DOI: 10.1142/9789812702517\_0096
- [17] A.G. Anisimov, A.D. Matrosov, G.A. Shvetsov. A. G. Anisimov, A. D. Matrosov, G. A. Shvetsov. *Journal of Applied Mechanics and Technical Physics*, **3** 375-379 (2002)
- [18] E.M. Drobyshevsky, E.N. Kolesnikova, V.S. Yuferev. *Technical Physics Letters*, **25** 260-262 (1999)
- [19] S.V. Bobashev, B.G. Zhukov, R.A. Kurakin, S.A. Ponyaev, B.I. Reznikov, S.I. Rozov. *Technical Physics*, **55** (12), 1754 & ndash; 1759 (2010).
- [20] V.A. Burtsev, N.V. Kalinin, A.V. Luchinskiy, *Elektricheskiy vzryv provodnikov i ego primeneniye v elektrofizicheskikh ustanovkakh* (Energoatomizdat, M., 1990) (in Russian).
- [21] A.N. Grigoriev, A.V. Pavlenko. *Technical Physics Letters*, **35**, 865 & ndash; 868 (2009).
- [22] V.M. Fomin, A.A. Golyshev, A.G. Malikov, A.A. Filippov, V.S. Shikalov, M.A. Yadrenkin, A.M. Orishich. *J. Eng. Phys. Thermophys.*, **95**, 1773 (2022). <https://doi.org/10.1007/s10891-022-02649-x>
- [23] V.M. Fomin, T.A. Brusentseva, A.A. Filippov, M.A. Yadrenkin, P.E. Tyustin. *J. Eng. Phys. Thermophys.*, **95** (7), 1659 (2022). <https://doi.org/10.1007/s10891-022-02635-3>
- [24] A. Malikov, A. Golyshev. *Materials*, **16**, 783 (2023). <https://doi.org/10.3390/ma16020783>
- [25] A. Golyshev, A. Malikov, I. Vitoshkin. *Crystals*, **13** (7), 1112 (2023). <https://doi.org/10.3390/cryst13071112>
- [26] M.A. Yadrenkin, R.E. Tyustin. *Features of High-Speed Microparticles Flow Accelerated by Railgun. XXI International Conference on the Methods of Aerophysical Research (ICMAR–2022)* (Novosibirsk, 8–14 Aug. 2022, Abstr. Pt.I. Novosibirsk: SB RAS, 2022), p. 210–211. [https://doi.org/10.53954/9785604788967\\_210](https://doi.org/10.53954/9785604788967_210)

Translated by 123